Second-order reflective-type, absorptive notch filter with lumped elements

Article *in* Microwave and Optical Technology Letters · November 2014

DOI: 10.1002/mop.28632

CITATIONS
2

READS
313

3 authors, including:

Andrei Grebennikov
Institute of Electrical and Electronics Engineers
180 PUBLICATIONS **2,210** CITATIONS

SEE PROFILE

soldered connector, which is about 12%, over five times larger as that in [6].

Measured gain of the proposed antenna using side soldered connector is shown in Figure 4, which agrees with the simulated result well in tendency. The peak gain is generated at near 10 GHz, where the resonances from the slots and patch both contribute to the radiation. After 10 GHz, radiation efficiency drops quickly due to only the patch radiating energy and beyond its operating frequency points.

Figure 5 shows the measured radiation pattern of the fabricated antenna using sider soldered connector in two orthogonal cut planes at 9.8, 10.0, and 10.2 GHz. It is found that a right hand circular polarization wave is generated.

4. CONCLUSION

We presented a new feeding transition method, namely stripline to SIW, for CP antenna design in this article. This feeding transition introduced several CP generations simultaneously to meliorate the AR bandwidth. By tuning the T-shape feeding line, we can make all of the modes couple each other properly. The design process for the proposed antenna is provided and the prototype of the recommended antenna is fabricated and measured. The experimental results demonstrated that the AR bandwidth is improved significantly to 12% compared with that in the published antennas.

REFERENCES

1. J. Hirokawa and M. Ando, Single-layer feed waveguide consisting of posts for plane tem wave excitation in parallel plates, IEEE Trans Antennas Propag 46 (1998), 625–630.
2. L. Yan, W. Hong, G. Hua, J. Chen, K. Wu, and T.J. Cui, Simulation and experiment on SIW slot array antennas, IEEE Microwave Wireless Compon Lett 14 (2004), 446–448.
3. Y.J. Cheng, W. Hong, and K. Wu, Design of a monopulse antenna using a dual v-type linearly tapered slot antenna (dvltsa), IEEE Trans Antennas Propag 56 (2008), 2903–2909.
4. G.Q. Luo, Z.F. Hu, L.X. Dong, and L.L. Sun, Planar slot antenna backed by substrate integrated waveguide cavity, IEEE Antennas Wireless Propag Lett 7 (2008), 236–239.
5. M. Bozzi, A. Georgiadis, and K. Wu, Review of substrate-integrated waveguide circuits and antennas, IET Microwaves Antennas Propag 5 (2011), 909–920.
6. D.-Y. Kim, J.W. Lee, T.K. Lee, and C.S. Cho, Design of SIW cavity-backed circular-polarized antennas using two different feeding transitions, IEEE Trans Antennas Propag 59 (2011), 1398–1403.
7. H. Wang, D.-G. Fang, B. Zhang, and W.-Q. Che, Dielectric loaded substrate integrated waveguide (SIW)-plane horn antennas, IEEE Trans Antennas Propag 58 (2010), 640–647.
8. P. Sharma and K. Gupta, Analysis and optimized design of single feed circularly polarized microstrip antennas, IEEE Trans Antennas Propag 31 (1983), 949–955.
9. S.D. Targonski and D.M. Pozar, Design of wideband circularly polarized aperture-coupled microstrip antennas, IEEE Trans Antennas Propag 41 (1993), 214–220.
10. H. Iwasaki, A circularly polarized small-size microstrip antenna with a cross slot, IEEE Trans Antennas Propag 44 (1996), 1399–1401.
11. C.-Y. Huang and K.-L. Wong, Coplanar waveguide-fed circularly polarized microstrip antenna, IEEE Trans Antennas Propag 48 (2000), 328–329.
12. D. Kim, J. Lee, C. Cho, and T. Lee, X-band circular ring-slot antenna embedded in single-layered SIW for circular polarisation, Electron Lett 45 (2009), 668–669.
13. S.A. Razavi and M.H. Neshati, Development of a low-profile circularly polarized cavity-backed antenna using hmsiw technique, IEEE Trans Antennas Propag 61 (2013), 1041–1047.
14. G.Q. Luo and L.L. Sun, Circularly polarized antenna based on dual-mode circular siw cavity, In: International Conference on Microwave and Millimeter Wave Technology 2008, pp. 1077–1079.
15. G.Q. Luo, Z.F. Hu, Y. Liang, L.Y. Yu, and L.L. Sun, Development of low profile cavity backed crossed slot antennas for planar integration, IEEE Trans Antennas Propag 57 (2009), 2972–2979.
16. K.-L. Wong, C.-C. Huang, and W.-S. Chen, Printed ring slot antenna for circular polarization, IEEE Trans Antennas Propag 50 (2002), 75–77.

SECOND-ORDER REFLECTIVE-TYPE, ABSORPTIVE NOTCH FILTER WITH LUMPED ELEMENTS

Senad Bulja, Pawel Rulikowski, and Andrei Grebennikov
Bell Labs Ireland, Alcatel-Lucent, Blanchardstown Industrial Park, Dublin, 15, Ireland; Corresponding author: senad.bulja@alcatel-lucent.com
Andrei Grebennikov is currently with RF Axis, Irvine, California 92618

Received 31 March 2014

ABSTRACT: *In this article, a design methodology and equations necessary for a second-order absorptive, reflective-type, transmission zero notch filter are introduced, derived, and described in detail. Initially, a single (first order), absorptive, reflective-type transmission zero notch filter is described. Based on this, improvements to the first-order reflective-type notch filter are discussed and a novel circuit that achieves a second-order absorptive, reflective-type, transmission zero notch response is proposed. The necessary conditions for the achievement of the second-order absorptive, reflective-type, transmission zero from the proposed circuit are derived. As an experimental verification, first- and second-order absorptive, reflective-type, transmission zero circuits are fabricated and their performance measured. It is shown that the first-order notch circuit introduces a zero into the response of a main filter with a depth of over 12 dB in the frequency range 2.19–2.27 GHz, while the second-order notch circuit introduces a transmission zero with a depth of over 20 dB GHz, in the same frequency range as its first-order counterpart.*
 Microwave Opt Technol Lett 56:2542–2545, 2014; View this article online at wileyonlinelibrary.com. DOI 10.1002/mop.28632

Key words: *filters; microstrip line; transmission zero; 3-dB coupler*

1. INTRODUCTION

Filters are omnipresent in virtually all communication systems. They are widely used in radar systems, point-to-point radio, earth stations, base stations, and repeaters. Even though the fundamental principles of filter theory have been known for a considerable time, practical filter design still draws a great deal of attention from RF engineers and academia.

However, one type of filtering solutions remains relatively unexplored and somewhat overlooked, especially for use in modern communication systems. The idea of absorptive filtering or leaky wall filtering was first introduced in [1], and was implemented using waveguide components. In general, absorptive filtering achieves attenuation by absorption, rather than reflection of the incident, travelling wave. In its simplest form, a leaky wall filter comprises simply of a cascade of slots in a rectangular [2] or coaxial [3] waveguide, which couple to a single auxiliary waveguide with absorptive end-loads. In view of this, the requirement for a highly selective absorptive filter, directly translates to the requirement of a highly selective notch

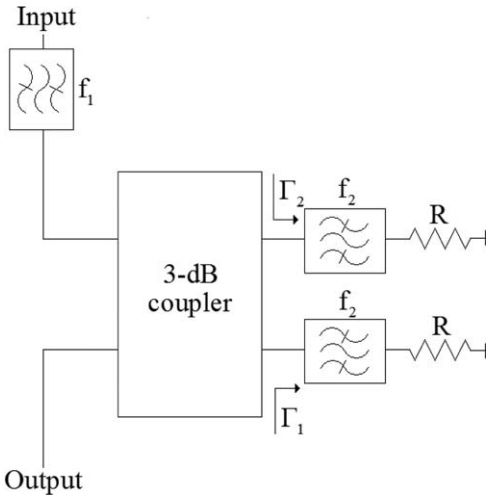

Figure 1 Simple absorptive filter with a first-order broadband transmission zero

filter, suitably coupled to the main filter. For the purpose of a notch filter, a reflective-type variant is particularly suitable when very low reflections are desired.

One such example is presented in [4]. The embodiment of this approach is shown in Figure 1. In this realization, a transmission zero is introduced into the response of filter f_1 by a notch filter structure that consists of a 3-dB coupler and filters f_2. The depth and width of the introduced first-order transmission zero is proportional to the reflection characteristics of filters f_2. The order of the transmission zero introduced in this way can be doubled by a cascade connection of two structures of Figure 1, however, such an arrangement will incur a high insertion loss, due to the presence of an extra 3-dB coupler and the interconnecting microstrip line between the two 3-dB couplers.

In this article, the circuit that enables the doubling of the order of a transmission zero in the reflective-type, absorptive configuration without increasing the number of 3-dB couplers is examined in detail. In particular, Section 2 describes the necessary theory and analysis of such a second-order, absorptive, reflective-type transmission zero notch filter, whereas Section 3 presents the experimental results.

2. THEORY AND ANALYSIS

The absorptive filter with a reflective-type configuration that enables a first-order transmission zero is presented in Figure 1. The operational principle is relatively simple. Pass-bands of filters f_1 and f_2 are arranged so the stop-band of filter f_1 overlaps with the pass-band of filter f_2. In this way, the signal existing in the stop-band of filter f_1 is greatly absorbed by parasitics of filters f_2 and terminating resistors R. Under the assumption of an ideal 3-dB coupler, the expressions for the reflection and transmission coefficients become [5]:

$$S_{11}=0.5(\Gamma_1-\Gamma_2) \quad \text{and} \quad S_{21}=-j0.5(\Gamma_1+\Gamma_2) \tag{1}$$

If the reflective loads are the same, that is, $\Gamma_1=\Gamma_2=\Gamma$, it follows that $S_{11}=0$ and $S_{21}=-j\Gamma$, that is, the reflection coefficient of filters f_2 now becomes the transmission coefficient of the overall absorptive filter. This result has the following two implications: first, filters f_2 can be lossy as it is their matching characteristic that influences the depth of the transmission zero, and second, due to the overlapping of the respective stop-band and pass-band of filters f_1 and f_2 and the fact that the incident signal power in the pass-band of filters f_2 is much lower than the incident signal power in the pass-band of filter f_1, filters f_2 can have a lower power rating, inferring the use of a low cost technology.

The depth of the first-order transmission zero introduced in this way is limited by the achievable impedance matching. Usually, an impedance matching between 10 and 15 dB is considered satisfactory in most cases. A better impedance match is usually more difficult to obtain, as it places stringent requirements on the tolerance of the components. Therefore, with reference to Figure 1, if a transmission zero deeper than 10–15 dB is required, an alternative solution to improved impedance matching needs to be sought, if lower tolerance components are to be used. As elaborated earlier, the replication of the notch circuits will inevitably double the depth of the introduced transmission zero, however, it will also increase the insertion loss.

A second-order transmission zero can be achieved with a reflective circuit of Figure 2 and 3 [6]. The reflective circuit consists of filters f_2 and lumped elements, X_1 and X_2, with input impedance, Z_{in}, given by

$$Z_{in}=\frac{2Z^3-2ZX_1X_2+Z(X_1+X_2)^2}{4Z^2+(X_1+X_2)^2}+j\left[\frac{(X_1+X_2)(X_1X_2+Z^2)}{4Z^2+(X_1+X_2)^2}\right] \tag{2}$$

First, it is necessary to impose the condition that the imaginary part of the input impedance is equal to zero, $\mathrm{Im}(Z_{in})=0$ so that the input impedance is purely real. Solving $\mathrm{Im}(Z_{in})=0$ yields the following relationship:

$$Z^2=-X_1X_2 \quad \text{or} \quad X_1=-X_2 \tag{3}$$

Using the latter substitution, as it results in a reduced form of the real part of the input impedance, one obtains

$$\Gamma=\frac{Z_{in}-Z_0}{Z_{in}+Z_0}=\frac{Z^2+Z(-2Z_0)+X_1^2}{Z^2+Z(2Z_0)+X_1^2} \tag{4}$$

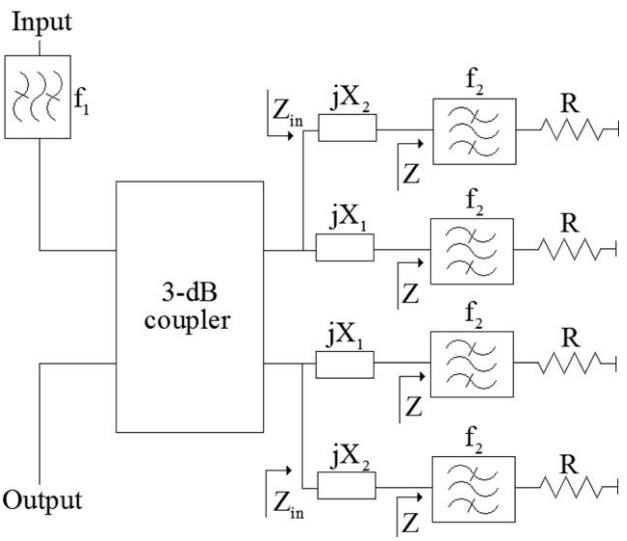

Figure 2 Absorptive filter with a second-order broadband transmission zero.

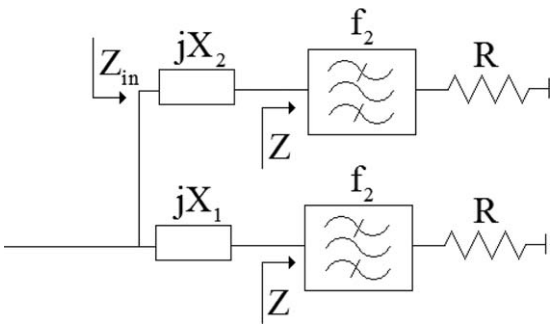

Figure 3 Reflective circuit of absorptive filter with a second-order broadband transmission zero

The second-order transmission zero is found from the condition that $\Gamma=0$, which yields

$$Z_{1,2}=\frac{2Z_0\pm\sqrt{4Z_0^2-4X_1^2}}{2} \tag{5}$$

The necessary condition for a second-order zero is achieved by requiring that the discriminant is equal to zero, which yields the value for the lumped element X_1, that is, $X_1=Z_0$. Once this condition is satisfied, a second-order zero is achieved at:

$$Z_{1,2}=Z_0 \tag{6}$$

And (4) can be rewritten as:

$$\Gamma=\frac{(Z-Z_0)(Z-Z_0)}{(Z+Z_0)(Z+Z_0)} \tag{7}$$

In this way, a second-order zero is achieved if the lumped elements are chosen in this fashion

$$Z=\pm X_1=\mp X_2=Z_0 \tag{8}$$

that is, the lumped elements have the reactances which magnitudes are equal to the characteristic impedance of the interconnecting lines, but of opposite signs.

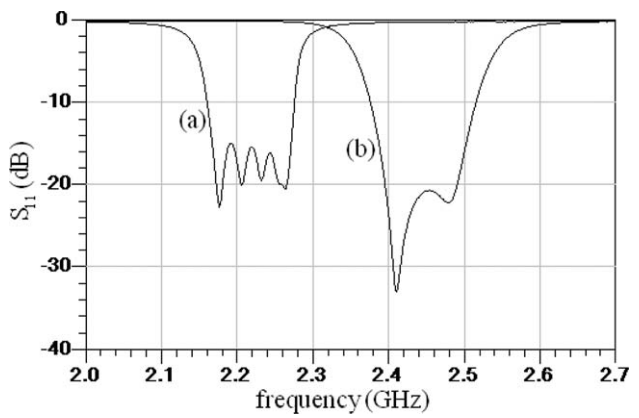

Figure 4 Reflection coefficient of (a) seventh-order in-house made Chebyshev filter and (b) CTS filter (CER0367A)

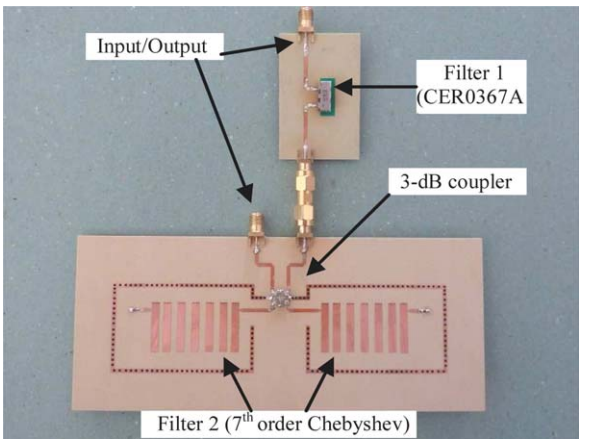

Figure 5 Photograph of a complete, absorptive filter with a first-order broadband transmission zero. [Color figure can be viewed in the online issue, which is available at wileyonlinelibrary.com]

3. RESULTS

To test the theory presented in the previous section, two absorptive filters were built. For this purpose, a filter from CTS, CER0367A, [7] is used as filter f_1. According to manufacturer's data, the filter exhibits a pass-band between 2.4 and 2.5 GHz. As filter f_2, an in-house made, seventh-order microstrip combine Chebyshev filter fabricated on a Roger Duroid TMM3 [8] substrate was used. This filter was made to operate in the frequency range between 2.19 and 2.27 GHz. The measured reflection coefficients of filters f_1 and f_2 are presented in Figure 4. The complete first- and second-order, transmission zero absorptive filters, are presented in Figures 5 and 6. As a 3-dB coupler, a quadrature surface mount hybrid coupler from Anaren [9], 1P603S, is used. This device operates across the frequency range of 2.3 to 2.7 GHz, with a maximum insertion loss of 0.3 dB. The values of the lumped inductor and capacitor necessary for the achievement of double transmission zero response were obtained using (8), to yield $C=1.43$ pF and $L=3.58$ nH, which, due to commercial availability of lumped element values were approximated by $C=1.3$ pF and $L=3.6$ nH. The measured transmission coefficients of the CTS

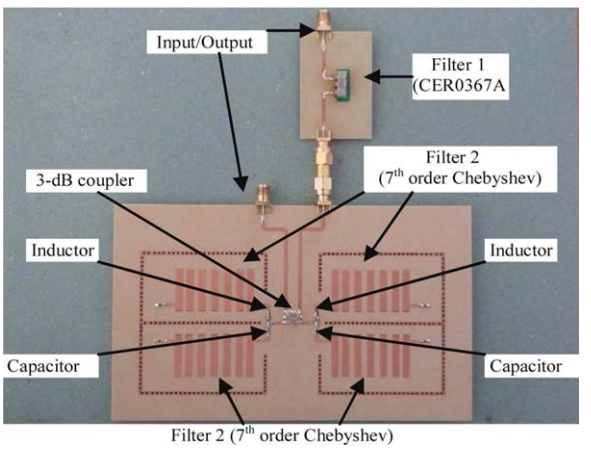

Figure 6 Photograph of a complete, absorptive filter with a second-order broadband transmission zero. [Color figure can be viewed in the online issue, which is available at wileyonlinelibrary.com]

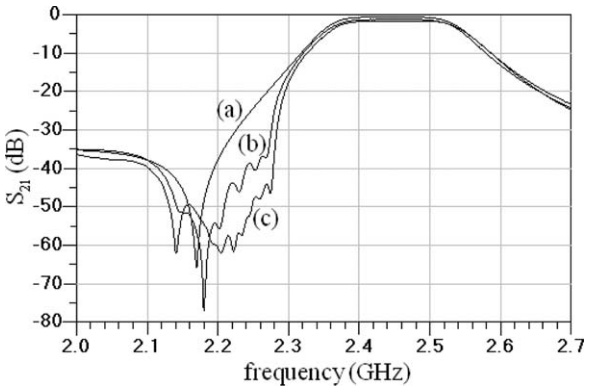

Figure 7 Transmission coefficient of (a) CTS CER0367A filter alone, (b) complete absorptive filter with first-order broadband transmission zero, and (c) complete absorptive filter with second-order broadband transmission zero

(CER0367A) filter and the absorptive filters of Figures 5 and 6 are given in Figure 7.

As evident from these figures, the first-order transmission zero circuit has introduced a transmission zero into the response of the main filter that is, CTS with a minimum depth of 12 dB in the frequency range of 2.19–2.27 GHz compared to the case of the CTS filter alone. The introduction of the single transmission zero has come at the expense of worsening the insertion loss in the pass-band of filter f_1 by 0.6 dB. This is contrasted by the second-order transmission zero of the circuit of Figure 6, which has further increased the depth of the transmission zero introduced by the circuit of Figure 5, so that the depth of the transmission zero in this case is over 20 dB in the frequency range of 2.19–2.27 GHz, when compared to the case of the CTS filter alone. It is believed that the depth of the transmission zero in this case can be further increased by a more careful choice of the lumped elements. Compared to the single transmission zero case, the insertion loss has been increased by 0.5 dB in the double transmission zero case.

4. CONCLUSION

In this article, a novel reflective-type circuit that enables the introduction of a second-order absorptive, transmission zero, notch filter response is presented. The equations governing the operation of the proposed circuit are also derived, so as to establish the potential of the proposed technique. The fabricated circuit offers a second-order transmission zero with a depth of over 20 dB in the frequency range of 2.19–2.27 GHz.

REFERENCES

1. V. Met, Absorptive filters for microwave harmonic power, Proc IRE 47 (1959), 1762–1769.
2. I.L. Powell, Waveguide filters, US Patent 3916352, October 28, 1975.
3. S. Conning, High-power harmonic suppression filters, US Patent 3496496, February 17, 1970.
4. P. Kenington, Duplexer and method for separating a transmit signal and a receive signal, Pub. No. US 2011/0080856 A1, April 7, 2011.
5. J. Reed and G.J. Wheeler, A method of analysis of symmetrical four-port networks, Proc IRE 4 (1956), 256–252.
6. S. Bulja and P. Rulikowski, Filter for RF applications, Patent pending (filed on July 4, 2013).
7. Available at: http://www.ctscorp.com, 2013.
8. Available at: http://www.rogerscorp.com, 2013.
9. Available at: http://www.anaren.com, 2013.

TRAPEZOIDAL RING QUAD-BAND FRACTAL ANTENNA FOR WLAN/WiMAX APPLICATIONS

V. Rajeshkumar and S. Raghavan
Department of Electronics and Communication Engineering, National Institute of Technology (NIT), Tiruchirappalli, Tamilnadu, India; Corresponding author: vrajeshme@gmail.com

Received 31 March 2014

ABSTRACT: *A novel multiband loaded trapezoidal ring fractal antenna (TRFA) is proposed for wireless local area network (WLAN) and worldwide interoperability for microwave access (WiMAX) applications. The self-similarity property is applied to the trapezoidal structure and the fractal geometry is achieved by consecutive iterations. The proposed antenna has a compact size of 30 × 30 × 1.6 mm^3. The antenna is fabricated and tested. The fourth iteration of the proposed TRFA covers the 2.4/5.2/5.8 GHz WLAN bands and 2.5/3.5/5.5 GHz WiMAX bands with uniform radiation characteristics and an average gain of 2.20 dBi.*
 Microwave Opt Technol Lett 56:2545–2548, 2014; View this article online at wileyonlinelibrary.com. DOI 10.1002/mop.28631

Key words: *fractal antenna; multiband; self similar; WiMAX; WLAN*

1. INTRODUCTION

The rapid growth in wireless communication demands for low cost, miniaturization, and compact multiband antennas. Multiband operation is one of the most important requirement for designing antennas used for multiple wireless communication systems, such as wireless local area network (WLAN) 2.4–2.484 GHz (specified by IEEE 802.11b/g) and 5.15–5.35/5.75–5.825 GHz (specified by IEEE 802.11a) and worldwide interoperability for microwave access (WiMAX) 2.5–2.69 GHz, 3.4–3.69 GHz bands (specified by IEEE 802.16e) and 5.25–5.85 GHz [1, 2]. In addition, the technologies like 2.4 GHz Bluetooth communication, WiFi (2.4–2.484 and 5.15–5.35 GHz), and RFID Tag Antenna (2.45GHz and 5.8GHz) also have great demands for compact multiband antenna systems.

The design method of multiband antennas involves various developed techniques. A multiband antenna can be obtained using multiresonators, defected ground plane structures, notched frequency bands, and fractal geometry techniques [2]. Fractal antennas are very compact, multiband or wideband and have useful applications in wireless communications. Recent studies proved that fractal antennas are more promising to satisfy the demands of multiband antenna systems [3, 4]. The space-filling and self-similar characteristics are the major key concepts behind the evolution of fractal antennas [5]. Several fractal geometries namely Minkowski, Sierpinski, Koch, and Hilbert geometries are successfully experimented for multiband applications [3–5]. In [6], a square-nested fractal antenna is designed by incorporating a series of similar square loops to cover the four bands of WLAN/WiMAX systems but with a larger antenna size. A compact microstrip-fed parasitic coupled ring fractal monopole antenna with semielliptical ground plane is presented for WLAN and WiFi applications [7]. In [8], fractal structures are used as radiating elements for the triband RFID reader/tag antenna with a larger size.

In several research articles, numerous fractal antennas are studied for multiband wireless communications [2–9]. Even though several wideband antennas have been designed to cover all the WLAN/WiMAX bands [1, 10], the multiband antennas